J. Fluid Mech. (1973), *vol.* 59, *part* 2, *pp.* 369–390
Printed in Great Britain

The effect of shear and stratification on the stability of a rotating fluid layer

By A. R. BRUNSVOLD† AND C. M. VEST
Department of Mechanical Engineering, The University of Michigan

(Received 30 October 1972)

The stability of a layer of Newtonian fluid confined between two horizontal disks which rotate with different angular velocities is studied. Both isothermal and adversely stratified fluids are considered for small shear rates at low to moderate Taylor numbers. The linearized formulation of the stability problem is given a finite-difference representation, and the resulting algebraic eigenvalue problem is solved using efficient numerical techniques. The critical parameters and disturbance orientations are determined as a function of the Taylor number for the isothermal flow, and for the stratified flow for Prandtl numbers of 0·025, 1·0 and 6·0.

At high Taylor numbers, the unstratified fluid flows in Ekman-like layers near the disks, and two modes of instability are noted: the viscous-type 'class A' travelling wave, whose existence depends on Coriolis forces, and the inflexional 'class B' mode, which is nearly stationary with respect to the nearer bounding disk. As the Taylor number is decreased, the Ekman layers coalesce to form a fully developed flow. In this regime there is a Taylor number below which the class A waves are always damped. The critical Reynolds number for the class B waves increases rapidly as the Taylor number approaches zero.

For Prandtl numbers of 1·0 and 6·0, the adversely stratified flow exhibits two distinct types of instability: convective and dynamical. At low Reynolds numbers, a stationary mode associated with Bénard convection in a rotating fluid is critical. It is stabilized and given orientation by the shear. At higher Reynolds numbers, the critical mode is a travelling wave of the nature of either the class A or class B waves, depending upon the Taylor number. For a Prandtl number of 0·025, the critical mode resembles oscillatory convection at small Reynolds numbers and a class A wave at larger shear rates.

1. Introduction

Shear, rotation, and density stratification all affect the stability of fluid flows with respect to small disturbances. In this paper a configuration is considered in which all three of these factors are present; namely, a layer of Newtonian fluid confined by two horizontal rotating disks which have different temperatures and different rotation rates. The significant parameters which specify this flow are the Taylor number T, the Reynolds number R, the Rayleigh number $\mathscr{R}$

† Present address: Argonne National Laboratory, Argonne, Illinois.

and the Prandtl number Pr. Linearized stability theory has previously been applied to several limiting cases of this configuration. The simplest case is the Bénard instability of a stationary fluid layer heated from below ($T = 0$, $R = 0$, $\mathscr{R} \neq 0$). Instability of this configuration occurs at a well-known critical Rayleigh number, and results in the formation of stationary convection cells. Analytical and experimental investigations of this problem are summarized by Chandrasekhar (1961). When the fluid layer heated from below rotates ($T \neq 0, R = 0, \mathscr{R} \neq 0$), instability may result in either stationary or oscillatory convection, depending on the values of T and Pr. Investigations of this problem are also summarized by Chandrasekhar (1961). When the fluid is not stratified and the mean rotation rate is zero ($T = 0, R \neq 0, \mathscr{R} = 0$), the present problem becomes equivalent to the stability analysis of plane Couette flow. This problem has been studied by several workers, including Hopf (1914), Wasow (1953), Zondek & Thomas (1953), Grohne (1954), Gallager & Mercer (1962), and Deardorff (1963). This flow appears to be stable at all R according to linearized theory. The case of plane Couette flow with adverse density stratification has been considered by Chandra (1938), Brunt (1951), Kuo (1963), Deardorff (1965), Gallager & Mercer (1965), Ingersoll (1966*a*, *b*) and others. These experimental and analytical studies show that small disturbances lead to stationary convection with the same critical Rayleigh number as the Bénard problem. The convection occurs as vortex rolls which are axially aligned with the base flow. Brunt (1951) and Ingersoll (1966*b*), in experimental investigations, observed some transverse rolls, but they are believed to have resulted from finite amplitude effects. Finally, if the fluid is unstratified but sheared ($T \neq 0$, $R \neq 0$, $\mathscr{R} = 0$), and if T is large, Ekman layers are formed near the boundaries. The stability of the Ekman layer has been studied experimentally by Faller (1963) and Tatro & Mollo-Christensen (1967) and analytically by Lilly (1966) and Faller & Kaylor (1966). The Ekman layer exhibits two travelling wave instabilities. One is a viscous-type instability, which is dependent upon the Coriolis force, and the other, which is nearly stationary with respect to the rotating disk, is an inflexional instability which can be predicted on the basis of inviscid theory. These modes are referred to as class A and class B waves, respectively.

In this paper the linearized stability analysis is extended into R, $\mathscr{R}$, T space in order to define the domain in which convective instabilities are critical and that in which dynamical instabilities are critical. Additional objectives are to determine the effect of reduced T and of stratification on the occurrence of class A and class B modes, and to determine the combined effect of shear and rotation on convective instability.

Recent work on the stability of stratified Ekman layers also deals with the combined effects of shear, rotation and stratification. Faller & Kaylor (1967) briefly discussed a study of the stability of both stably and adversely stratified Ekman layers by numerical solution of the corresponding initial-value problems. For the case of adverse stratification, the initial configuration considered was one of cellular convection in a fluid layer of finite depth above a rotating disk. In these numerical experiments, the vortex rolls due to instability of the Ekman layer were observed to compete with the convection cells for dominance; the

outcome depended on the values of R and $\mathscr{R}$. The study of the stably stratified configuration was extended and presented by Kaylor & Faller (1972). It was found that, at large Richardson numbers, resonance can occur between the boundary-layer instability and internal gravity waves. This can cause an increase in disturbance growth rate with increasing Richardson number. At lower Richardson numbers, stable stratification has a damping effect.

Etling (1971) and Brown (1972) have also studied the stability of the stratified Ekman layer. Etling, using a finite-difference formulation of the stability problem, found considerable destabilization of the Ekman layer due to adverse stratification. Stable stratification has a damping effect, which is particularly strong for the class B inflexional mode. He also found that inclusion of the vertical component of vorticity in the analysis renders the critical Reynolds number a function of the orientation of the mean flow. Brown concentrated his study on the disturbances having maximum growth rates at supercritical Reynolds numbers. The Coriolis force was neglected in the computations, which were thereby limited to the class B inflexional modes. Unstable stratification was found to shift the maximum growth rate disturbances towards a longitudinal orientation and to decrease their wavelength from that for the unstratified flow.

In the study reported here, the model of the base flow is based on an analysis by Stewartson (1953) of the isothermal flow between rotating disks. He used the assumption, introduced by Von Kármán (1921) and Batchelor (1951), that the axial velocity is a function of only the axial co-ordinate. The mean temperature profile is taken to be linear, and the parameter range in which this model of the base flow is realistic is assessed. Essentially, the study is limited to small shear rates and low to moderate Taylor numbers. A finite-difference representation of the differential system governing infinitesimal wave-like disturbances in a localized region of the flow is developed. This transforms the stability analysis into an algebraic eigenvalue problem, which is solved numerically. Plots of the critical parameters, including wavenumber and orientation, as functions of the Taylor number are presented for the unstratified flow and for stratified flows with $Pr = 0{\cdot}025$, $1{\cdot}0$ and $6{\cdot}0$. These curves are shown to approach the known results for the various limiting cases discussed above.

2. Base flow

Consider the flow of a Newtonian fluid confined between two horizontal coaxial disks of infinite extent. The bottom disk rotates at a rate Ω_1, and the upper disk at a different rate Ω_2, about the z axis, which is parallel to the gravity vector and positive upward. The disks are each isothermal, but of different temperatures, T_1 for the bottom disk and T_2 for the upper disk. When the transport properties are considered to be constant and viscous dissipation and work of compression are neglected, the Boussinesq equations, written in a rotating reference frame with origin at the midplane, are

$$\nabla . \hat{\mathbf{V}} = 0, \tag{2.1}$$

$$\frac{D\hat{\mathbf{V}}}{D\hat{t}} + 2\Omega \mathbf{k} \times \hat{\mathbf{V}} = -\frac{1}{\rho}\nabla \hat{P} + \nu \nabla^2 \hat{\mathbf{V}} - \frac{\beta \Omega^2}{2} \nabla |\mathbf{k} \times \hat{\mathbf{r}}|^2 \hat{\theta} + \beta g \hat{\theta} \mathbf{k}, \tag{2.2}$$

$$D\hat{\theta}/D\hat{t} = \kappa\nabla^2\hat{\theta}, \tag{2.3}$$

where
$$\hat{P} = \hat{P}_0 + \rho g\mathbf{k} - \tfrac{1}{2}\rho\Omega^2|\mathbf{k}\times\hat{\mathbf{r}}|. \tag{2.4}$$

Here $\hat{P}_0$ is the hydrostatic pressure, $\hat{\theta}$ is the excess temperature above ambient, Ω is the rotation rate of the fluid at the midplane $z = 0$, ρ is the density, ν is the kinematic viscosity, β is the volume expansivity, g is the gravitational acceleration and κ is the thermal diffusivity. It is desired to obtain a representation of the steady axisymmetric base flow which is valid for small differences in rotation rates of the disks and low to moderate mean rotation rates.

When the variables are non-dimensionalized as

$$\left.\begin{aligned}[\hat{r},\hat{z}] = [r_0 r, Lz], \quad [\hat{V}_r,\hat{V}_\theta,\hat{V}_z] = U_0[V_r,V_\theta,V_z],\\ \hat{P} = \rho U_0^2 P, \quad \hat{\theta} = \Delta T\theta,\end{aligned}\right\} \tag{2.5}$$

where $U_0 = \frac{1}{2}(\Omega_2 - \Omega_1)r_0 \equiv \epsilon r_0$ is the characteristic shear velocity, $\Delta T = T_1 - T_2$, r_0 is the local radius, L is the separation of the disks and a carat denotes dimensional quantities, the dimensionless governing equations in cylindrical coordinates become

$$\frac{L}{r_0}\frac{1}{r}\frac{\partial(rV_r)}{\partial r} + \frac{\partial V_z}{\partial z} = 0, \tag{2.6}$$

$$\frac{\epsilon}{\Omega}\left[V_r\frac{\partial V_r}{\partial r} - \frac{V_\theta^2}{r} + \frac{r_0}{L}V_z\frac{\partial V_r}{\partial z}\right] - 2V_\theta = -\frac{\epsilon}{\Omega}\frac{\partial P}{\partial r} + \frac{1}{T}\left[\left(\frac{L}{r_0}\right)^2\mathscr{L}(V_r) + \frac{\partial^2 V_r}{\partial z^2}\right] - \frac{\beta\Delta T}{\epsilon/\Omega}r\theta, \tag{2.7}$$

$$\frac{\epsilon}{\Omega}\left[V_r\frac{\partial V_\theta}{\partial r} + \frac{V_r V_\theta}{r} + \frac{r_0}{L}V_z\frac{\partial V_\theta}{\partial z}\right] + 2V_r = \frac{1}{T}\left[\left(\frac{L}{r_0}\right)^2\mathscr{L}(V_\theta) + \frac{\partial^2 V_\theta}{\partial z^2}\right], \tag{2.8}$$

$$\frac{\epsilon}{\Omega}\left[V_r\frac{\partial V_z}{\partial r} + \frac{r_0}{L}V_z\frac{\partial V_z}{\partial z}\right] = -\frac{\epsilon}{\Omega}\frac{r_0}{L}\frac{\partial P}{\partial z} + \frac{1}{T}\left[\left(\frac{L}{r_0}\right)^2\frac{1}{r}\frac{\partial}{\partial r}\left(r\frac{\partial V_z}{\partial r}\right) + \frac{\partial^2 V_z}{\partial z^2}\right] + \frac{\beta\Delta T g}{(\epsilon/\Omega)\,\Omega^2 r_0}\theta, \tag{2.9}$$

$$RPr\left[\frac{L}{r_0}V_r\frac{\partial\theta}{\partial r} + V_z\frac{\partial\theta}{\partial z}\right] = \left(\frac{L}{r_0}\right)^2\frac{1}{r}\frac{\partial}{\partial r}\left(r\frac{\partial\theta}{\partial r}\right) + \frac{\partial^2\theta}{\partial z^2}, \tag{2.10}$$

and must be solved subject to the boundary conditions

$$\left.\begin{aligned}V_\theta/r = (\Omega_1 - \Omega)/\epsilon, \quad V_r = V_z = 0, \quad \theta = 0 \quad \text{at} \quad z = -\tfrac{1}{2},\\ V_\theta/r = (\Omega_2 - \Omega)/\epsilon, \quad V_r = V_z = 0, \quad \theta = -1 \quad \text{at} \quad z = \tfrac{1}{2},\end{aligned}\right\} \tag{2.11}$$

where the operator $\mathscr{L}$ is defined by

$$\mathscr{L} = \frac{\partial^2}{\partial r^2} + \frac{1}{r}\frac{\partial}{\partial r} - \frac{1}{r^2} \tag{2.12}$$

and where $T = \Omega L^2/\nu$. The latter quantity is referred to in this paper as the Taylor number.

For an isothermal (*unstratified*) fluid, $\theta \equiv 0$, and the energy equation (2.10) need not be considered. Following Von Kármán (1921) and Batchelor (1951), the class of solutions for which

$$V_z = V_z(z) \tag{2.13}$$

is considered. It then follows from (2.6)–(2.9) that

$$V_\theta/r = \tilde{u}(z), \quad V_r/r = \tilde{v}(z), \tag{2.14}$$

where $\tilde{u}$ and $\tilde{v}$ are functions of z only. From (2.6),

$$V_z = -2\frac{L}{r_0}\int \tilde{v}(T^{\frac{1}{2}}z)\,dz + \text{constant} = -\frac{L}{r_0}T^{-\frac{1}{2}}W(T^{\frac{1}{2}}z), \tag{2.15}$$

where W is as yet undetermined and $T^{-\frac{1}{2}}$ is introduced for convenience. The momentum equations then reduce to

$$\frac{\epsilon}{\Omega}[\tilde{v}^2 - \tilde{u}^2 - T^{-\frac{1}{2}}W\tilde{v}'] - 2\tilde{u} = -\frac{\epsilon}{\Omega}\frac{1}{r}\frac{\partial P}{\partial r} + T^{-1}\tilde{v}'', \tag{2.16}$$

$$(\epsilon/\Omega)\,[2\tilde{u}\tilde{v} - T^{-\frac{1}{2}}W\tilde{u}'] + 2\tilde{v} = T^{-1}\tilde{u}'' \tag{2.17}$$

and

$$T^{-\frac{1}{2}}\left(\frac{L}{r_0}\right)^2\left[\frac{\epsilon}{\Omega}WW' + W''\right] = -\frac{\epsilon}{\Omega}\frac{\partial P}{\partial z}. \tag{2.18}$$

By noting that the pressure must be of the form $P = r^2P_1 + P_2(z)$, where P_1 is a constant, and assuming small shear, $\epsilon/\Omega \ll 1$, the system can be further simplified to give

$$\tilde{v}''' + 2T\tilde{u}' = 0, \quad \tilde{u}''' - 2T\tilde{v}' = 0. \tag{2.19}$$

A simple solution to this set of equations was given by Stewartson (1953), who defined a complex quantity $\tilde{Z} = \tilde{u} + i\tilde{v}$, which must satisfy

$$\tilde{Z}''' - (1-i)^2 TZ' = 0. \tag{2.20}$$

The solution of (2.20) with the appropriate boundary conditions, and with the requirement of no net radial flow, is

$$\tilde{Z} = \frac{\sinh T^{\frac{1}{2}}(1-i)z}{\sinh \frac{1}{2}T^{\frac{1}{2}}(1-i)}. \tag{2.21}$$

The usefulness of this solution depends on the extent of the parameter range in which the linearization of the equations, based on $\epsilon/\Omega \ll 1$, is reasonable and also on the physical reality of Von Kármán's and Batchelor's assumption, equation (2.13). Comparison of (2.21) with Lance & Roger's (1962) numerical solution of the nonlinear equations (2.16)–(2.18) for $\epsilon/\Omega = \frac{1}{3}$ and various T indicates reasonable agreement even at Taylor numbers as high as $T = 126$. For $T \leqslant 18{\cdot}6$ the solutions of the linear and nonlinear equations are virtually identical. For Taylor numbers in the range $18{\cdot}6 < T < 126$, the general shape of the linearized solution (2.21) is correct; however, there is some discrepancy in that, as T increases, the nonlinear solution indicates that the fluid at the midplane no longer rotates at $\Omega = \frac{1}{2}(\Omega_1 + \Omega_2)$, as in equation (2.21). The experimental investigations of Schultz-Grunow (1935), Stewartson (1953) and Picha & Eckert (1958) indicate that, if the disks are shrouded (so that the fluid which travels radially is re-ingested into the flow), the velocity is in agreement with solutions based on the assumption (2.13). The velocity given by Stewartson's (1953) solution, equation (2.21), was used in the study of the stability of the unstratified fluid flow reported here, and is considered to be essentially correct for $T \lesssim 100$ if $\epsilon/\Omega \lesssim 1$.

In the case of *stratified* flows, consideration must be given to the last term in (2.7). This term represents the *excess centrifugal force*, which always causes some

convective flow if there is a density gradient parallel to the axis of rotation. The parameter $\beta\Delta T(\epsilon/\Omega)^{-1}$, which appears in this term, is a measure of the ratio of the excess centrifugal acceleration due to stratification to the Coriolis acceleration. If

$$\frac{\beta\Delta T}{\epsilon/\Omega} \ll 1, \tag{2.22}$$

the excess centrifugal force can therefore be neglected, since Coriolis effects will have time scales significantly shorter than those for the term in question. The neglect of this term is further justified if the Froude number $Fr = \Omega^2 r_0/g$, which is a measure of the ratio of the excess centrifugal force to the buoyancy force, is small. It is relevant to note that experimental results for Bénard instability in the presence of rotation are in good agreement with the theory which ignores this term, even though $Fr > 1$. The excess centrifugal force is ignored here in both the base-flow and stability analyses, which are considered to be subject to the restriction of equation (2.22).

For the stratified base flow, the assumption of Von Kármán and Batchelor, equation (2.13), is again made since the r- and θ-momentum equations are only weakly and indirectly coupled to the energy equation through the pressure gradient. It then follows that $P = r^2 P_1 + P_2(z)$ and $\theta = \theta(z)$, so the energy equation (2.10) can be written as

$$\frac{d^2\theta}{dz^2} + \frac{\epsilon}{\Omega} Pr\, T^{\frac{1}{2}} W \frac{d\theta}{dz} = 0, \tag{2.23}$$

where W, as yet undetermined, is related to V_z by (2.15). Since $d\theta/dz \to -1$ as $(\epsilon/\Omega)\, Pr\, T^{\frac{1}{2}} \to 0$, equation (2.23) can be integrated once to yield

$$\frac{d\theta}{dz} = -\exp\left[-\frac{\epsilon}{\Omega} Pr\, T^{\frac{1}{2}} \int W\, dz\right]. \tag{2.24}$$

Letting $T^{-\frac{1}{2}} W_1(T^{\frac{1}{2}} z)$ denote $\int W(T^{\frac{1}{2}} z)\, dz$, then

$$\begin{aligned} \frac{d\theta}{dz} &= -\exp\left[-\frac{\epsilon}{\Omega} Pr\, W_1(T^{\frac{1}{2}} z)\right] \\ &= -\left[1 - \frac{\epsilon}{\Omega} Pr\, W_1(T^{\frac{1}{2}} z) + \left(\frac{\epsilon}{\Omega}\right)^2 Pr^2\, W_1^2(T^{\frac{1}{2}} z) + \ldots\right], \end{aligned} \tag{2.25}$$

where $(\epsilon/\Omega)\, Pr$ is assumed to be small. Hence, for small shear, $\epsilon/\Omega < 1$, the temperature gradient of the base flow can be taken as $d\theta/dz = -1$, with an error of order $(\epsilon/\Omega)\, Pr$. The velocity of the stratified base flow is then taken to be given by (2.21). This representation of the base-flow velocity and temperature is assumed to be reasonably accurate when $\epsilon/\Omega < 1$, $T \lesssim 100$, $\beta\Delta T(\epsilon/\Omega)^{-1} \ll 1$ and $(\epsilon/\Omega)\, Pr T^{-\frac{1}{2}} \ll 1$; and also without these restrictions if $T \to 0$ or $R \to 0$.

3. Stability analysis

The equations governing a small wave-like disturbance are obtained by the usual perturbation procedure. The dimensional velocity, for example, is represented as the sum of the base-flow and disturbance velocities:

$$\hat{\mathbf{V}}(\hat{x},\hat{y},\hat{z},\hat{t}) = \hat{\bar{\mathbf{V}}}(\hat{y},\hat{z}) + \epsilon'\hat{\mathbf{V}}'(\hat{x},\hat{y},\hat{z})\exp\{i\alpha(\hat{y}-\sigma\hat{t})\}, \tag{3.1}$$

where ϵ' is a small quantity and all velocities are referred to a local co-ordinate system (x,y,z) whose origin is located at an arbitrary radius r_0. In general, the form (3.1) requires that a global description of the disturbance velocity $\hat{\mathbf{V}}'$ be specified; however, on the basis of experimental observations and analyses of several other physical problems which are intimately related to the present one, it is assumed that the stability of the flow depends essentially on the *local* conditions. For example, Gregory, Stuart & Walker (1955) showed this to be the case in an experimental and theoretical study of the stability of the flow near a single rotating disk. Also, Faller (1963) and Tatro & Mollo-Christensen (1967) observed that instabilities of the Ekman layer occur as inward-travelling horizontal vortex rolls whose widths are of the same order as the boundary-layer thickness. In the case of the Bénard problem with and without rotation, instability leads to formation of convection cells of characteristic dimensions of the order of the plate spacing. In addition, the observations of Chandra (1938), Brunt (1951), Ingersoll (1966*b*) and others indicate that shear tends simply to align such motions, yielding convective rolls, rather than cells, while maintaining essentially the same characteristic dimension. With these facts in mind, the instability of the flow at $r_0 \gg L$ is analysed by treating the velocities $\hat{\bar{\mathbf{V}}}$ and $\hat{\mathbf{V}}'$ at r_0 as functions only of $\hat{z}$. If curvature is neglected, by dropping all terms of order L/r_0, the dimensionless disturbance equations are found to be

$$\left.\begin{aligned} \nabla_1^4\phi - i\alpha R\{(\tilde{v}-c/R)\nabla_1^2\phi - (D^2\tilde{v})\phi\} - 2TDu - i\alpha Gr\theta &= 0,\\ \nabla_1^2 u - i\alpha R\{(\tilde{v}-c/R)u - (D\tilde{u})\phi\} + 2TD\phi &= 0,\\ \nabla_1^2\theta - i\alpha RPr(\tilde{v}-c/R)\theta - i\alpha Pr\phi &= 0, \end{aligned}\right\} \tag{3.2}$$

where $D = d/dz$, $\nabla_1^2 = (D^2-\alpha^2)$ and $c = (L/\nu)\sigma$. The parameters in these equations are $R = U_0 L/\nu$, the local Reynolds number, $T = \Omega L^2/\nu$, the Taylor number, $Gr = \beta g \Delta T L^3/\nu^2$, the Grashof number, and $Pr = \nu/\kappa$, the Prandtl number. In the derivation of these equations, the non-dimensionalization

$$\left.\begin{aligned} [\hat{x},\hat{y},\hat{z}] &= [r_0 x, r_0 y, Lz],\\ [\hat{\bar{\mathbf{V}}},\hat{\mathbf{V}}'] &= [U_0\bar{\mathbf{V}}, (\nu/L)\mathbf{V}],\\ \hat{P}' &= \rho_0 U_0(\nu/L)P,\\ [\hat{\bar{\theta}},\hat{\theta}'] &= [\Delta T\bar{\theta}, \Delta T\theta] \end{aligned}\right\} \tag{3.3}$$

was used, and a stream function ϕ defined by

$$w = -i\alpha\phi, \quad v = \partial\phi/\partial y \tag{3.4}$$

was introduced. Since vortex roll disturbances are anticipated, the local co-ordinate system has been oriented such that the x axis is aligned with the axis of

the vortex at an angle γ measured counterclockwise from the azimuthal direction. In this skewed co-ordinate system, the base-flow velocity components are

$$\left.\begin{aligned} \tilde{u} &= \tilde{u}_1 \cos\gamma + \tilde{v}_1 \sin\gamma, \\ \tilde{v} &= -\tilde{u}_1 \sin\gamma + \tilde{v}_1 \cos\gamma, \end{aligned}\right\} \tag{3.5}$$

where

$$\left.\begin{aligned} \tilde{u}_1 &= (A \sinh T^{\frac{1}{2}}z \cos T^{\frac{1}{2}}z + B \cosh T^{\frac{1}{2}}z \sin T^{\frac{1}{2}}z)/(A^2+B^2), \\ \tilde{v}_1 &= (-B \sinh T^{\frac{1}{2}}z \cos T^{\frac{1}{2}}z + A \cosh T^{\frac{1}{2}}z \sin T^{\frac{1}{2}}z)/(A^2+B^2), \end{aligned}\right\} \tag{3.6}$$

with $A = \sinh \frac{1}{2}T^{\frac{1}{2}} \cos \frac{1}{2}T^{\frac{1}{2}}$ and $B = \cosh \frac{1}{2}T^{\frac{1}{2}} \sin \frac{1}{2}T^{\frac{1}{2}}$. The base temperature distribution is

$$\bar{\theta} = -\tfrac{1}{2}(1+2z). \tag{3.7}$$

The disturbance must satisfy the boundary conditions

$$\phi = D\phi = u = \theta = 0 \quad \text{at} \quad z = \pm\tfrac{1}{2} \tag{3.8}$$

if the bounding disks are rigid and highly conducting.

Numerical analysis

The differential system (3.2) and (3.8) constitutes an eigenvalue problem. For fixed values of the parameters R, T, Gr, Pr, α and γ, solutions for the eigenfunctions ϕ, u and θ are admitted only for certain values of c, the complex eigenvalue. A finite-difference scheme, similar to that used by Lilly (1966) in his study of the stability of the Ekman layer, was used to replace the differential system by an algebraic system. The z domain was divided into N intervals, and the eigenfunctions were expanded in Taylor series about the interior nodes, ϕ and θ being defined at nodal points and u being defined at half-nodes. Using a centred difference scheme,

$$\left.\begin{aligned} D\phi &= \delta\phi_j - \tfrac{1}{24}\Delta^2\delta^3\phi_j + \ldots, \\ D^2\phi &= \delta^2\phi_j - \tfrac{1}{12}\Delta^2\delta^4\phi_j + \ldots, \\ D^4\phi &= \delta^4\phi_j - \tfrac{1}{6}\Delta^2\delta^6\phi_j + \ldots, \end{aligned}\right\} \tag{3.9}$$

where $\Delta = 1/N$, $\delta\phi_j = (\phi_{j+\frac{1}{2}} - \phi_{j-\frac{1}{2}})/\Delta$, $\delta^2\phi_j = \delta(\delta\phi_j)$, etc., equations (3.2), along with the boundary conditions (3.8), were reduced to a homogeneous set of $3N-2$ linear algebraic equations in $3N-2$ unknowns. To minimize truncation errors, the *remainder terms* (those of $O(\Delta^2)$) were retained in the expansions of all terms except those of the highest order derivative in each equation. Base-flow quantities were computed at nodal, or half-nodal, points using (3.6) and (3.7). The resulting algebraic eigenvalue problem can be represented in matrix form as

$$[\mathbf{C}^{-1}[\mathbf{A} + i\mathbf{B}] - \lambda\mathbf{I}] \begin{Bmatrix} \phi \\ u \\ \theta \end{Bmatrix} = 0, \tag{3.10}$$

where $\mathbf{I}$ is the unit matrix and

$$\lambda = -i\alpha(c^r + ic^i) \tag{3.11}$$

is an eigenvalue. The elements of the complex submatrices $\mathbf{A}$, $\mathbf{B}$ and $\mathbf{C}$ are given in detail by Brunsvold (1972).

The eigenvalues of (3.10) were in general computed by converting the matrix to the Hessenberg, upper almost triangular, form by similarity transformations and then applying the LR iteration, described by Wilkinson (1965, p. 485), to the transformed matrix. This was accomplished using efficient Fortran-IV versions of the programs COMBAL, COMHES and COMLR, which were originally given in ALGOL by Parlett & Reinsch (1969) and Martin & Wilkinson (1968*a*, *b*).

In some regions of the parameter space, the neutral disturbance is stationary ($c^r = 0$), so that at neutral stability $\lambda = 0$. In this case, vanishing of the determinant $|\mathbf{A}+i\mathbf{B}|$ is a necessary and sufficient condition for neutral stability, so neutrally stable states of this type were located by finding the zeros of this determinant. This is significantly more economical than computing the eigenvalues of the matrix. To evaluate the determinant, a complex version of a routine described by Moler (1971), for real determinants, was written. This routine uses Gaussian elimination and partial pivoting in an LU decomposition which completes the interchanges in U but only partially completes the interchanges in L. Unlike many Gaussian reduction programs, Moler's routine uses primarily column operations; this substantially reduces subscript calculations and repetitive addressing of widely separated locations. In the virtual memory system which was used (the University of Michigan MTS), this resulted in significant savings of time, owing to a large reduction in the number of paging operations.

All numerical results presented in this paper are believed to have converged to within about 0·5 % of their limiting values as N is increased. Checks on computational accuracy were made by studying numerical convergence to known results for various limiting cases such as the Bénard problem ($T = 0, R = 0, \mathscr{R} \neq 0$), the Bénard problem with rotation ($T \neq 0$, $R = 0$, $\mathscr{R} \neq 0$) and plane Couette flow heated from below ($T \to 0$, $R \neq 0$, $\mathscr{R} \neq 0$), where $\mathscr{R} = GrPr$ is the Rayleigh number. On the basis of the various convergence studies which were made, the calculations presented below were made with $25 \leqslant N \leqslant 40$. Details of the convergence studies are reported by Brunsvold (1972).

Although a detailed investigation of the effect of including the remainder terms in the finite-difference representation was not made over the entire range of parameters, sample calculations showed that it significantly increases computational efficiency. For example, at fairly small N ($15 \leqslant N \leqslant 25$), it was found that inclusion of the remainder terms improved convergence of the critical parameters to the correct value by about 3 % which is greater than the improvement due to a decrease of mesh size, which doubled the computational time.

The effect of shear

To study the effect of shear on the stability of a layer of unstratified (isothermal) fluid confined between rotating disks, the differential system (3.2) and (3.8) was simplified by setting $Gr = 0$ and deleting the thermal energy equation. The matrix form of the corresponding finite-difference representation, equation (3.10), is then reduced to order $2N-1$. The locus of neutrally stable states, $\lambda^r = 0$, is a surface in T, R, α, γ space. The objective of the numerical study was to locate the critical states (defined here as those neutral states having the lowest value

of the Reynolds number for a fixed Taylor number) in the R, T plane and to determine the corresponding wavenumber and orientation.

Computations to locate the critical states were performed in conversational mode with the computer. A trace of the growth rate λ^r as a function of α at constant R and T was generated until the region of maximum growth rate was roughly located. A second growth-rate curve was then generated at a new value of α. From these two curves, both α and the minimum value of R at neutral stability could be estimated. For these values of α and R, a similar procedure was carried out while varying the orientation γ. This procedure was repeated iteratively until α, γ and R were known at the critical state. When necessary, the entire iteration scheme was repeated with successively finer mesh sizes until convergence appeared to be satisfactory.

Table 1 is a summary of the parametric study. Two distinct instabilities were found. Following Greenspan's (1968, p. 276) discussion of the stability of the Ekman layer and related rotational flows, these are denoted as class A waves and class B waves. The B waves, which are nearly stationary with respect to the rotating disks, are inflexional instabilities whose general characteristics can be determined by inviscid theory. This was done by Stuart in Gregory, Stuart & Walker (1955). The A waves were shown by Lilly (1966) to depend on a more complicated mechanism involving the Coriolis and shear forces.

To facilitate comparison of the present results with the existing literature on rotating fluids, the behaviour of the base flow and its instability for large T must be considered. On referring the velocity, equation (2.21), to that of the bottom disk, using Ω_1 as the reference rotation rate, and taking the limit as $T \to \infty$, the base velocity becomes

$$\bar{\mathbf{V}}(\xi) = \hat{\mathbf{i}}_1\{1 - e^{-\xi}\cos\xi\} + \hat{\mathbf{i}}_2 e^{-\xi}\sin\xi, \tag{3.12}$$

where

$$\xi = T^{\frac{1}{2}}(\tfrac{1}{2} + z) \tag{3.13}$$

and $\hat{\mathbf{i}}_1$ and $\hat{\mathbf{i}}_2$ are unit vectors in the azimuthal and radially inward directions, respectively. Equation (3.12) is recognized as the Ekman spiral. The continuity equation, when expressed in terms of the stretched co-ordinate ξ, suggests that $U_0/T^{\frac{1}{2}}$ is the appropriate velocity scale; hence a new Reynolds number $R_\epsilon = R/T^{\frac{1}{2}}$ is defined. Similarly, the disturbance quantities $u_\epsilon = u/T^{\frac{1}{2}}$ and $\alpha_\epsilon = \alpha/T^{\frac{1}{2}}$ are introduced. The appropriate form of the disturbance equations as $T \to \infty$ can then be deduced (Brunsvold 1972):

$$\nabla_1^4\phi - i\alpha_\epsilon R_\epsilon\{(\tilde{v}_\epsilon - c_\epsilon)\nabla_1^2\phi - D^2\tilde{v}_\epsilon\phi\} - 2Du = 0, \tag{3.14}$$

$$\nabla_1^2 u - i\alpha_\epsilon R_\epsilon\{(\tilde{v}_\epsilon - c_\epsilon)u - D\tilde{u}_\epsilon\phi\} + 2D\phi = 0, \tag{3.15}$$

subject to

$$\left.\begin{aligned} \phi = D\phi = u = 0 \quad &\text{at} \quad z = 0, \\ \phi = D^2\phi = Du = 0 \quad &\text{as} \quad z \to \infty, \end{aligned}\right\} \tag{3.16}$$

where $c_\epsilon = (c/R) - \sin\gamma$. Equations (3.14) and (3.15) are the stability equations of the Ekman layer, as given by Lilly (1966). Although (3.14) and (3.15) were not used in this study, this discussion suggests that the stability results should be presented in terms of R_ϵ, α_ϵ and c_ϵ to facilitate comparison with known results for the instability of the Ekman layer. This has been done in table 1.

T	Wave type	R	R_c	α	α_c	γ (deg)	c^r/R	c_c
100·0	*A*	563	56·3	3·24	0·324	−20·0	0·226	0·568
100·0	*B*	1105	110·5	5·10	0·510	10·0	0·238	0·065
70·0	*A*	533	62·5	2·75	0·329	−16·5	0·226	0·472
70·0	*B*	931	111·3	4·40	0·527	10·5	0·239	0·057
50·0	*A*	774	109·0	1·83	0·259	−9·0	0·236	0·394
50·0	*B*	856	121·0	3·90	0·550	13·0	0·247	0·023
48·46	*A*	855	122·8	1·70	0·244	−8·0	0·238	NC†
48·46	*B*	851	122·0	3·85	0·552	13·0	0·248	NC
35·0	*B*	956	161·4	3·15	0·531	18·0	0·267	NC
20·0	*B*	4805	1074·0	1·15	0·258	35·0	0·359	NC

† Not calculated.

TABLE 1. Critical parameters for unstratified flow

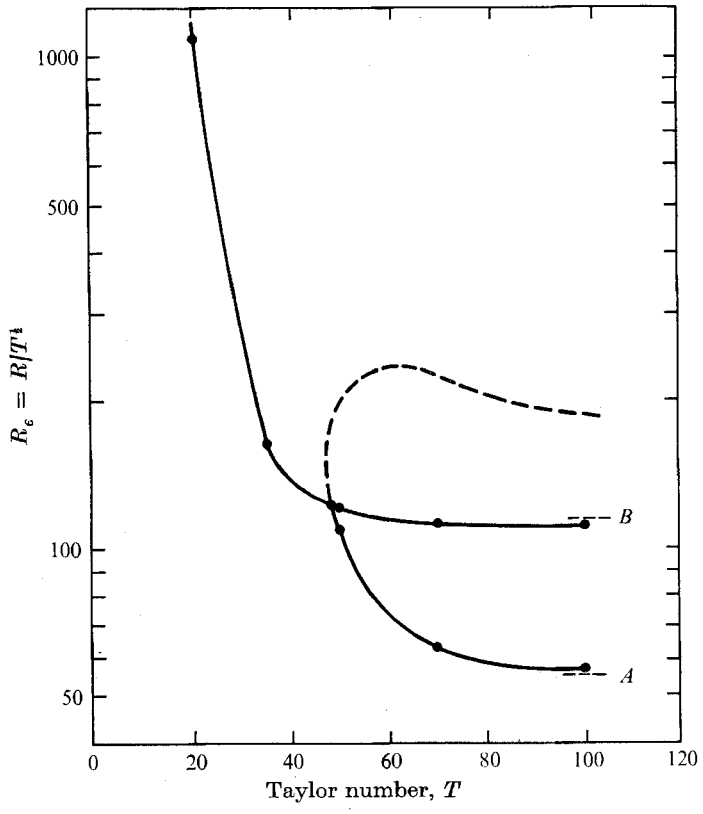

FIGURE 1. Critical Reynolds numbers for the class *A* and class *B* instabilities of the unstratified flow.

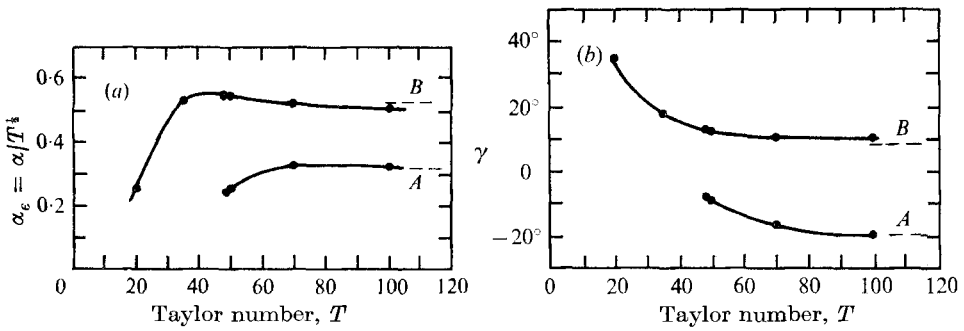

FIGURE 2. Critical parameters for the class A and class B instabilities of the unstratified flow. (*a*) Critical wavenumber. (*b*) Critical orientation.

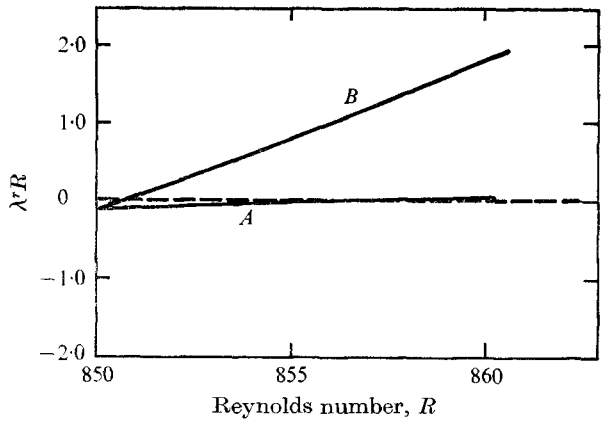

FIGURE 3. Growth rates of the class A and class B instabilities of the unstratified flow near the critical R for $T = 48{\cdot}64$.

Figure 1 is a plot of the critical R_c as a function of T. The critical wavenumber and orientation are shown in figure 2. Lilly's (1966) results for the class A and class B waves are indicated as dashed asymptotes in these figures. At $T = 100$ the critical Reynolds numbers of the present study are within 3% of Lilly's value for the A wave and within 4% for the B wave. As the Taylor number is decreased, the Ekman layers grow in the z direction and coalesce to form a fully developed velocity profile. Both A and B type instabilities still occur. Below $T = 47$, however, the A wave can no longer be sustained. A thorough numerical search was carried out at $T = 45$. Vestiges of the A wave were recognized, but it was always damped. This is consistent with Lilly's (1966) indication that the growth of class A disturbances can be supported only through the Coriolis forces, which are measured by T. The upper region of the critical curve for the A wave is shown qualitatively as a dashed line in figure 1, because detailed calculations were not made in this region. It is known, from Lilly's work for $T \to \infty$, that the A wave is not amplified at $R_c = 500$, but the exact value of the upper bound is not known.

Figure 3 shows the growth rates of the A and B waves at $T = 48{\cdot}64$, which is close to the intersection of the critical curves for these two instabilities. The

B wave has the larger growth rate at slightly supercritical R_c and therefore, within the limitation of linear theory, would be expected to dominate in a real flow. Faller (1963) and Tatro & Mollo-Christensen (1967), however, have found experimentally that both waves may coexist in the same Ekman-layer flow, although the class A waves can occur at smaller R_c.

As T is decreased below 47 the critical Reynolds number increases rapidly, and apparently without bound. As $T \to 0$, the base velocity profile becomes linear and equations (3.2) reduce to the Orr–Sommerfeld equation if the orientation is $\gamma = 90°$. The rapid increase of critical Reynolds number is therefore compatible with the linear-theory studies of plane Couette flow by Gallager & Mercer (1962) and Deardorff (1963), for finite R, and those of Hopf (1914), Wasow (1953), Zondek & Thomas (1953) and Grohne (1954), for $\alpha R \to \infty$, all of which suggest that the flow is stable at all finite values of R. Furthermore, the trends of the wave speeds and orientations given here are consistent with the conclusions of Hopf (1914) and Grohne (1954) that, for the disturbance with minimum damping, $c^r/R \to \pm 1$ (and $\gamma = \pm 90°$) as $\alpha R \to \infty$. Since the trend was clear, computations were not carried out for $T < 20$, where the critical R becomes so large that very fine meshes are required to achieve sufficient spatial resolution of the eigenfunctions.

The effect of stratification

To study the combined effects of shear and stratification on the stability of a layer of fluid confined between rotating disks, the entire differential system (3.2) and (3.8), or its finite-difference representation (3.10), must be considered. The locus of neutrally stable states is now a surface in T, R, Gr, Pr, α, γ space. The objective of the numerical study was to locate the critical states in the Gr, R plane with T and Pr as parameters. In this discussion a critical state is that neutral state which has the minimum Grashof number for fixed Reynolds, Taylor and Prandtl numbers.

The computational procedure used when the critical disturbance was not stationary is equivalent to that described in the discussion of the effect of shear, except that there are additional parameters in the present case.

In a large region of the parameter space considered, the critical disturbances were found to be stationary convective rolls and could therefore be located by finding the zeros of the determinant $|\mathbf{A} + i\mathbf{B}|$. For fixed values of all parameters other than Gr, the zero of the determinant was bracketed to within an interval of about 1 % of the value of Gr. α was then varied until Gr was roughly minimized. Using this value of α, Gr was then minimized with respect to γ. The entire procedure was iterated until the critical state was located. Since these critical states were determined under the assumption that $\lambda = 0$, the results were checked at sample locations by computing the eigenvalues of (3.10), to ensure that the stationary mode was indeed the critical one.

The results of the numerical study for $Pr = 6{\cdot}0$ and $Pr = 1{\cdot}0$ are presented in tables 2 and 3, and are represented graphically in figures 4 and 5. These curves of critical parameters were drawn using the numerical data in tables 2 and 3. Additional information regarding the trends of these curves was obtained from

T	R	R_c	Gr	α	γ (deg)	c^r/R
100·0	100·0	10·0	2638·0	5·80	17·5	0
100·0	200·0	20·0	3854·5	5·65	−2·5	0
100·0	300·0	30·0	5154·8	6·10	−13·0	0
100·0	500·0	50·0	7435·5	6·50	−21·0	0
50·0	50·0	7·07	1242·7	4·65	68·0	0
50·0	200·0	28·28	3701·5	4·85	49·5	0
50·0	500·0	70·70	8334·9	5·55	40·5	0
50·0	730·0	103·2	5000·0	1·90	−10·0	0·231
20·0	50·0	11·2	683·2	3·40	−61·5	0
20·0	200·0	44·8	2982·4	4·50	−71·0	0
20·0	500·0	111·8	7283·5	5·05	−75·0	0

TABLE 2. Critical parameters for stratified flow (Pr = 6·0)

T	R	R_c	Gr	α	γ (deg)	c^r/R
100·0	100·0	10·0	9905·0	5·56	74·0	0
100·0	200·0	20·0	12540·0	5·08	67·0	0
100·0	300·0	30·0	16199·0	5·33	50·0	0
100·0	400·0	40·0	19268·0	5·56	37·0	0
100·0	500·0	50·0	21998·0	5·68	31·0	0
100·0	559·0	55·9	15000·0	3·35	−20·0	0·211
70·0	100·0	11·9	7208·0	4·80	86·0	0
70·0	300·0	35·8	14666·0	4·70	66·0	0
70·0	500·0	59·7	22230·0	5·10	51·0	0
50·0	50·0	7·07	4777·5	4·55	−82·0	0
50·0	200·0	28·28	9622·0	3·70	−87·0	0
50·0	500·0	70·70	25247·0	5·00	69·0	0
50·0	738·0	104·3	14000·0	1·92	−10·5	0·225
50·0	756·0	112·0	7000·0	1·88	−10·0	0·228
35·0	50·0	8·45	3660·0	4·05	−69·0	0
35·0	200·0	33·8	9370·0	2·90	−69·0	0
35·0	500·0	84·5	27663·0	5·30	87·0	0
35·0	947·0	160·0	5000·0	3·13	18·0	0·266
20·0	50·0	11·2	2610·0	3·50	−49·0	0
20·0	100·0	22·4	3709·0	3·30	−48·0	0
20·0	200·0	44·8	8675·0	2·50	−49·0	0
20·0	300·0	67·1	15176·0	5·00	−58·0	0
20·0	500·0	111·8	25415·0	5·85	−64·0	0

TABLE 3. Critical parameters for stratified flow (Pr = 1·0)

preliminary computations of lower accuracy. Those regions in which there is significant uncertainty regarding the precise structure of the curve are indicated by dashed lines. Discontinuities which occur upon transition from convective to dynamical instability as the critical mode are denoted by dot–dashed lines.

At $T = 0$, the problem reduces to the classical Bénard problem, so the critical curves are simply the straight lines $Gr = 1708/Pr$. For non-zero T and $R = 0$, the problem reduces to the Bénard problem with rotation, which has been studied extensively by Chandrasekhar (1953) and Chandrasekhar & Elbert (1955), and

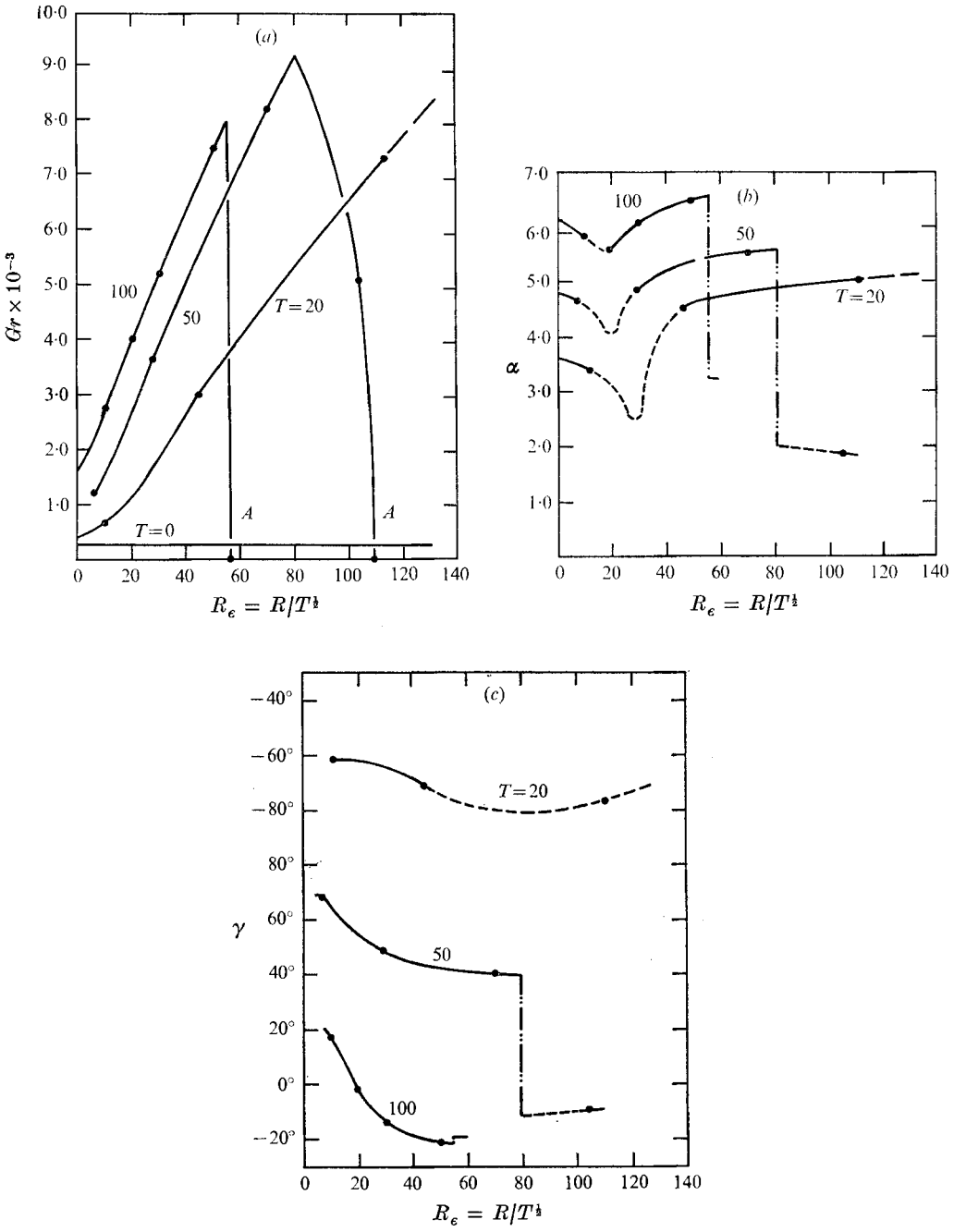

FIGURE 4. (*a*) Critical Grashof numbers, (*b*) critical wavenumbers for $Pr = 6{\cdot}0$ and (*c*) critical orientation angles (in degrees) for $Pr = 6{\cdot}0$.

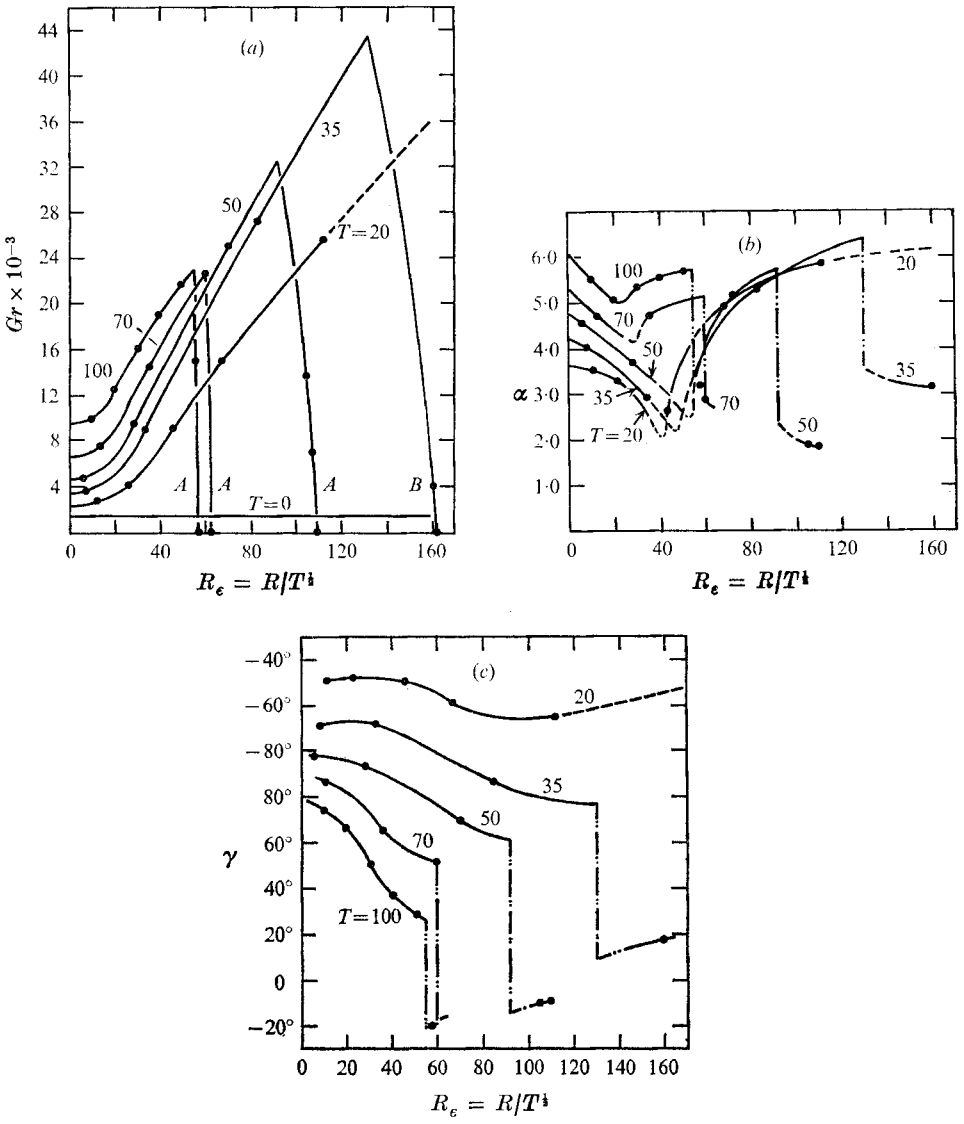

FIGURE 5. (*a*) Critical Grashof numbers, (*b*) critical wavenumbers and (*c*) critical orientation angles (in degrees) for $Pr = 1{\cdot}0$.

summarized by Chandrasekhar (1961). Convergence of the results of the present study to those given in the latter reference was within 0·5 %. (It should be noted that Chandrasekhar's (1961) results are given in terms of a different Taylor number $Ta = 4T^2$.) The linear theory is considered to be accurate in the Taylor number range considered here; however, at higher T, Veronis (1959, 1966), Rossby (1969), Niiler & Bisshopp (1965) and Homsey & Hudson (1971*a*, *b*) have shown that the excess centrifugal force, formation of Ekman-like layers and nonlinear phenomena become important. For $Pr = 1{\cdot}0$ and $Pr = 6{\cdot}0$ the critical disturbances at $R = 0$ are in the form of stationary convection cells with no preferred orienta-

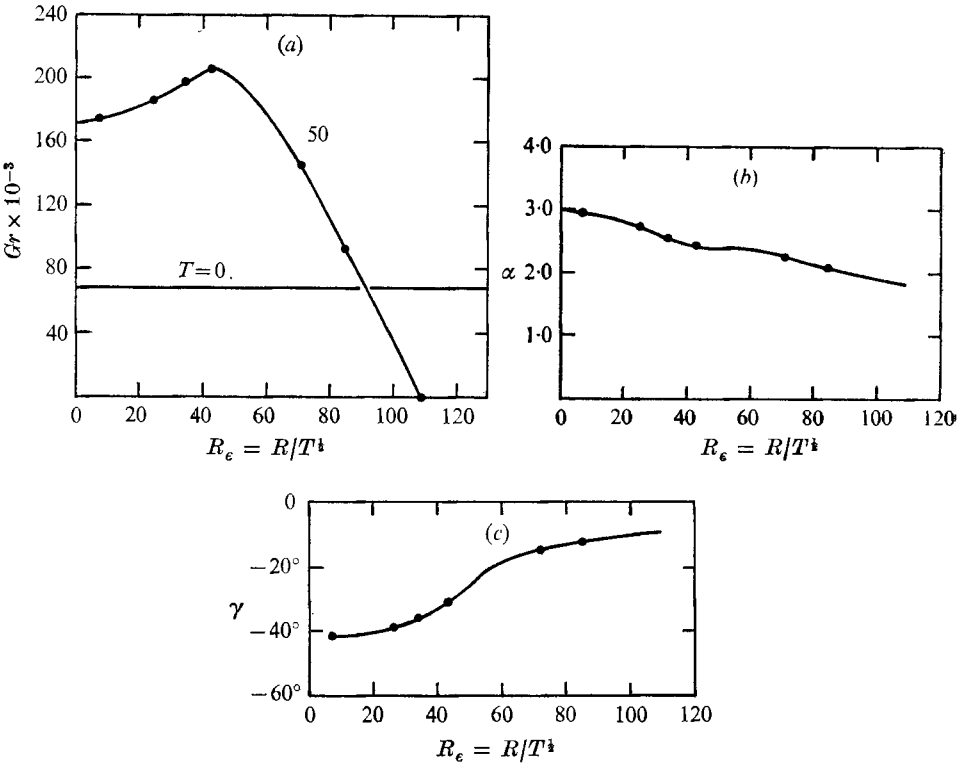

FIGURE 6. (*a*) Critical Grashof numbers, (*b*) critical wavenumbers ($T = 50$) and (*c*) critical orientation angles (in degrees, $T = 50$) for $Pr = 0{\cdot}025$.

tion. When the shear, as measured by $R_c = R/T^{\frac{1}{2}}$, is increased, the critical disturbances appear as stationary convective roll vortices with specific orientations. As indicated in figure 5(*a*), shear, in the presence of rotation, has a stabilizing effect on these stationary disturbances. Increasing T at fixed R_c also stabilizes the flow. As R_c is increased further, travelling wave modes become more critical than the stationary modes. The points of transition from one mode to the other as the critical one are indicated by discontinuities in the critical parameter curves. The travelling waves are again denoted by A and B since they have the same characteristics as the class A and class B waves which occur in the unstratified flow ($Gr = 0$). The A waves are critical when $T \gtrsim 47$ and the B waves are critical when $T \lesssim 47$. Rotation, as measured by T, has a destabilizing influence on the travelling wave modes. Shear, as measured by R_c, has a similar destabilizing influence. Sample computations also indicate that the neutral curves for the travelling wave modes follow the same trend into the domain of negative Gr as that shown in figure 5(*a*) for $Gr > 0$. That is, stable stratification appears to have a damping influence on the dynamical modes.

The critical curves for $Pr = 0{\cdot}025$ (figures 6) are somewhat different since all critical disturbances are non-stationary at this Pr. The numerical results, computed for $T = 50$, were all obtained by calculating the eigenvalues of (3.10). They are given in table 4. As $R \to 0$ the problem is reduced to that of the Bénard

T	R	R_c	Gr	α	γ (deg)	c^r/R
50·0	50·0	7·07	173800·0	2·93	−41·5	0·332
50·0	175·0	24·77	186200·0	2·70	−39·0	0·141
50·0	240·0	34·3	197300·0	2·51	−36·0	0·135
50·0	300·0	42·4	204900·0	2·41	−31·5	0·144
50·0	500·0	70·7	144900·0	2·25	−15·0	0·206
50·0	600·0	84·8	92600·0	2·09	−12·5	0·233

TABLE 4. Critical parameters for stratified flow (Pr = 0·025)

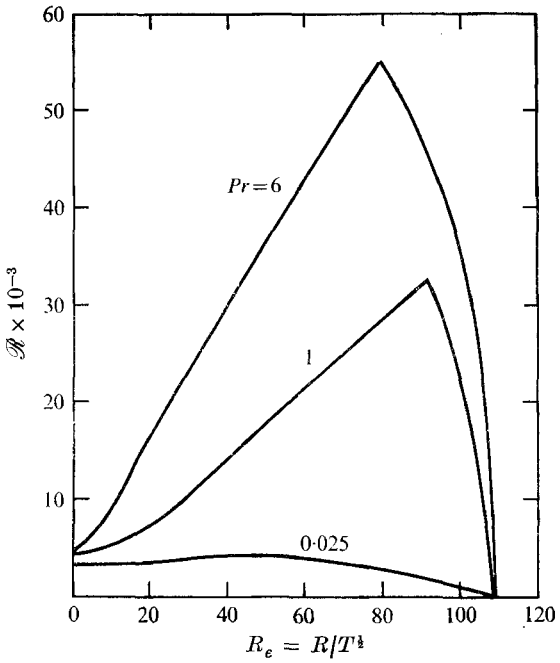

FIGURE 7. Critical Rayleigh numbers at T = 50 for various Prandtl numbers.

instability with rotation. Chandrasekhar (1953) and Chandrasekhar & Elbert (1955) found for the case of *free* boundaries that the critical disturbances are overstable for Pr = 0·025 if $T \gtrsim 12$. In the present study (see appendix), it was found that with *rigid* boundaries the critical disturbance is overstable if $T \gtrsim 45$.

The critical Gr is seen in figure 6(*a*) to at first increase as R_c is increased and then to decrease until the critical curve crosses the R_c axis at the A wave critical state of the unstratified flow. The critical wavenumbers and orientations are indicated in figures 6(*b*) and (*c*). None of these critical curves appear to have abrupt discontinuities as in the case of Pr = 1·0 and Pr = 6·0. The imaginary part λ^i of the eigenvalue also seemed to be a rather smooth function of R_c. Thus it appears that these curves may become continuous in the limit $Pr \to 0$. It would be of interest to pursue this point in greater detail.

The results for all three Prandtl numbers are compared at T = 50 in figure 7. If the Rayleigh number $\mathscr{R} = Gr\,Pr$ is considered as the critical parameter, Pr

is seen to have a stabilizing influence in the presence of rotation and shear. This is compatible with Gallager & Mercer's (1965) and Ingersoll's (1966*a*) studies of plane Couette flow heated from below, which indicated that Pr has a stabilizing influence on disturbances with transverse components.

4. Discussion

The stability of a layer of Newtonian fluid confined between two horizontal disks which rotate with different angular velocities has been studied using a linearized analysis. A simple base-flow model which is valid for low to moderate Taylor numbers and small shear rates was used. Instabilities resembling both the viscous-type class A mode and the inflexional-type class B mode, which occur in the Ekman layer, were found to exist in the developed flow considered here. Indeed, the critical parameters for these modes closely approach their Ekman-layer values at Taylor numbers sufficiently low to be within the domain of validity of this simple base flow ($T = \Omega L^2/\nu \lesssim 100$). For $T \gtrsim 47$, the class A mode is the more critical of the two; however, previous experimental studies of the Ekman layer suggest that both modes may coexist in a real flow. For $T \lesssim 47$, the class A mode, which Lilly (1966) showed to be sustained by a complex mechanism involving Coriolis as well as viscous forces, is always damped. The class B waves continue to exist at low Taylor numbers, although the critical Reynolds number appears to grow indefinitely as $T \to 0$. This is as expected since the configuration approaches plane Couette flow in this limit.

If an adverse stratification is introduced, by heating the fluid layer from below, the critical modes at low Reynolds numbers are convective instabilities. Hence for low R_c, the investigation can be characterized as a study of the effect of shear on Bénard instability in a rotating fluid. Shear was found to stabilize the configuration with respect to the stationary convective vortices which are critical for $Pr = 1{\cdot}0$ and $Pr = 6{\cdot}0$, and also to affect the orientation of these vortices. It was found that, at low R_c, the vortices are aligned with the base-flow velocity vector close to the centre of the layer ($z \sim 0{\cdot}25$), rather than with the azimuthal direction of the strong flow near the boundaries. Since convective vortices in non-rotating shear flows are known to be aligned with the base velocity, this suggests that the vortices may be confined to the core region of the flow. This supposition is supported by the increase in wavenumber as the base flow tends towards a boundary-layer structure with increasing T. Furthermore, as R_c increases at fixed T, the orientation corresponds to the base velocity even further into the core region. This would appear to be consistent with the cutting off of convection cells by the boundary-layer shear flow at high R_c, which was observed in Faller & Kaylor's (1967) numerical studies of the stratified Ekman layer.

As the Reynolds number is increased with fixed Pr and T, the dynamical modes (A or B) eventually become critical. Adverse stratification has a destabilizing influence on these modes. A similar destabilization was noted by Etling (1971) in a study of the adversely stratified Ekman layer. He found large decreases in critical Reynolds numbers as a 'stratification parameter' was

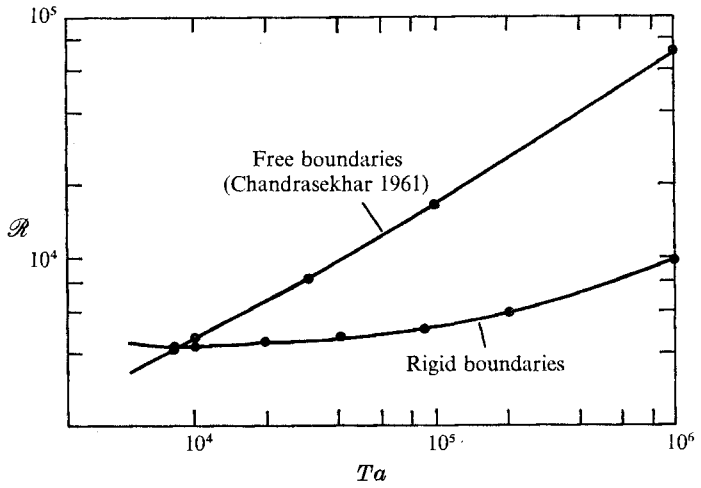

FIGURE 8. Critical Rayleigh numbers for Bénard instability with rotation (rigid boundaries), $Pr = 0{\cdot}025$,

increased. For the present configuration it was found that the convective instability generally becomes critical before a large reduction in the critical R_c of the dynamical modes has been realized.

The nature of the problem for $Pr = 0{\cdot}025$ is somewhat different because, even in the absence of shear, the convective instability is oscillatory, rather than stationary. Shear was still found to stabilize the convective mode at small R_c and to destabilize the dynamical mode at larger R_c. Unlike the cases of $Pr = 1{\cdot}0$ and $6{\cdot}0$, the values of the critical parameters did not seem to suffer abrupt changes as the critical mode switched from being convective to dynamical. This suggests that there may be a smooth transition in the limit $Pr \to 0$.

The authors wish to acknowledge the useful discussions with Professor V. S. Arpaci and Professor C. B. Moler, and to express their appreciation for the computer time which was donated by The University of Michigan Computer Center and the Department of Mechanical Engineering.

Appendix. A note regarding Bénard instability with rotation

Chandrasekhar (1953) and Chandrasekhar & Elbert (1955) have presented discussions of the stability of a horizontal rotating fluid layer heated from below. This work, along with other results, is summarized by Chandrasekhar (1961). Detailed information is presented for the case in which both bounding surfaces are free (no shear stress). Some computations, based on a variational principle, are also reported for the case of rigid boundaries. It is known (cf. Chandrasekhar 1961) that, for free boundaries, neutral disturbances are oscillatory (overstable) if $Pr < 0{\cdot}67$ and if $Ta = 4\Omega^2 L^2/\nu^2$ is sufficiently large. For mercury, $Pr = 0{\cdot}025$, the system is overstable at critical $\mathscr{R}$ if $Ta \gtrsim 608$, and becomes unstable with respect to stationary disturbances otherwise. In the present study, it was

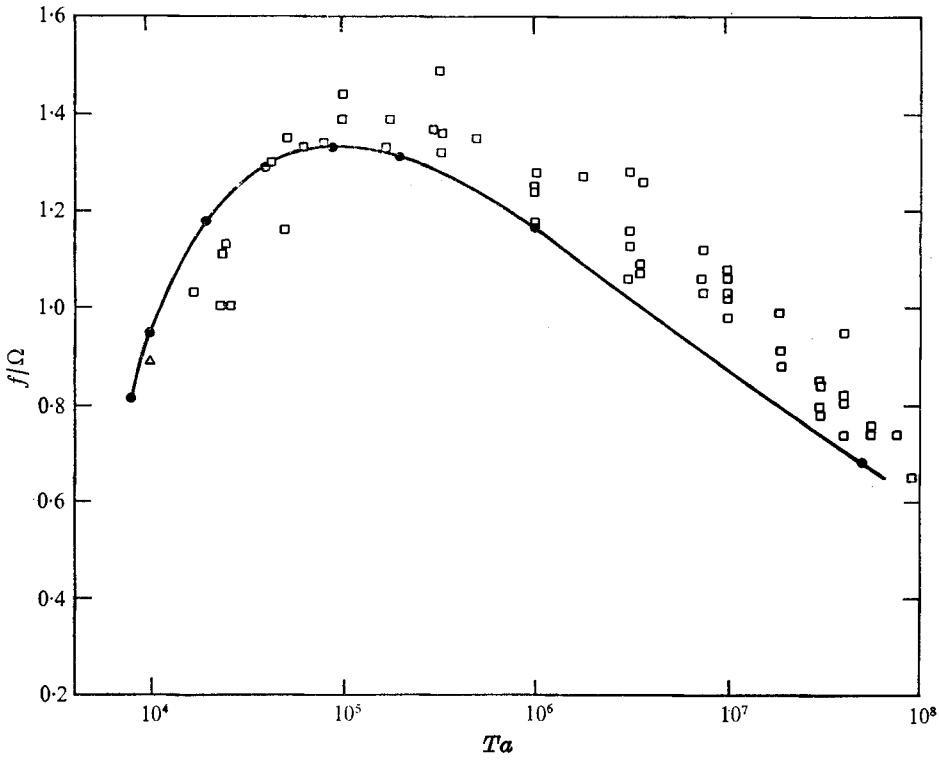

FIGURE 9. Critical frequencies of Bénard instability with rotation (rigid boundaries), and comparison with the data of Rossby (1969), $Pr = 0{\cdot}025$. ●, present study; □, experiment (Rossby 1969); △, calculation (Chandrasekhar 1961).

desirable to know accurately at what Ta this transition occurs if the bounding surfaces are rigid. Critical states for oscillatory disturbances were determined using iterative eigenvalue computations similar to those described in this paper. The variation of the critical $\mathscr{R}$ with Ta is shown in figure 8, along with the results of Chandrasekhar (1961) for stationary disturbances. It was found that the critical disturbances are oscillatory if $T \gtrsim 45$ and stationary if $T \lesssim 45$.

The frequency, $f/\Omega = \lambda^i/T$, of the critical disturbances was also computed in the Taylor number range $8100 < Ta < 10^6$. These computations were made because it was pointed out by Rossby (1969) that no such detailed calculations were available with which his experimental data for mercury could be compared. This range is of particular interest because the scatter of Rossby's data about an estimated frequency curve suggests poor agreement with linear theory. Such a result would indeed be compatible with the finite amplitude instability considerations of Veronis (1959, 1966). The linear-theory results of the present study are shown, along with Rossby's data, in figure 9. Although the data appear to fit this curve somewhat better than they fit the extrapolation of Chandrasekhar's (1961) results, which was used by Rossby, the data scatter still switches from above the curve to below it at $Ta \sim 5 \times 10^4$. Hence Rossby's discussion of this parameter region appears to remain valid in light of these calculations.

REFERENCES

BATCHELOR, G. K. 1951 *Quart. J. Mech. Appl. Math.* **4**, 29.

BROWN, R. A. 1972 *J. Atmos. Sci.* **29**, 850.

BRUNSVOLD, A. R. 1972 Ph.D. dissertation, The University of Michigan.

BRUNT, D. 1951 In *Compendium of Meteorology*, p. 1255. Am. Meteor. Soc.

CHANDRA, K. 1938 *Proc. Roy. Soc.* A **164**, 231.

CHANDRASEKHAR, S. 1953 *Proc. Roy. Soc.* A **217**, 306.

CHANDRASEKHAR, S. 1961 *Hydrodynamic and Hydromagnetic Stability*. Oxford University Press.

CHANDRASEKHAR, S. & ELBERT, D. D. 1955 *Proc. Roy. Soc.* A **231**, 198.

DEARDORFF, J. W. 1963 *J. Fluid Mech.* **15**, 623.

DEARDORFF, J. W. 1965 *Phys. Fluids*, **8**, 1027.

ETLING, D. 1971 *Beitr. Phys. Atmos.* **44**, 168.

FALLER, A. J. 1963 *J. Fluid Mech.* **15**, 560.

FALLER, A. J. & KAYLOR, R. 1966 *J. Atmos. Sci.* **23**, 466.

FALLER, A. J. & KAYLOR, R. 1967 *Phys. Fluids Suppl.* **10**, S212.

GALLAGER, A. P. & MERCER, A. McD. 1962 *J. Fluid Mech.* **13**, 91.

GALLAGER, A. P. & MERCER, A. McD. 1965 *Proc. Roy. Soc.* A **286**, 117.

GREENSPAN, H. P. 1968 *The Theory of Rotating Fluids*. Cambridge University Press.

GREGORY, N., STUART, J. T. & WALKER, W. S. 1955 *Phil. Trans. Roy. Soc.* A **248**, 155.

GROHNE, D. 1954 *Z. angew. Math. Mech.* **35**, 344.

HOMSEY, G. M. & HUDSON, J. L. 1971*a* *J. Fluid Mech.* **45**, 353.

HOMSEY, G. M. & HUDSON, J. L. 1971*b* *J. Fluid Mech.* **48**, 605.

HOPF, L. 1914 *Ann. Phys., Lpz.* **44**, 1.

INGERSOLL, A. P. 1966*a* *Phys. Fluids*, **9**, 862.

INGERSOLL, A. P. 1966*b* *J. Fluid Mech.* **25**, 209.

KAYLOR, R. & FALLER, A. J. 1972 *J. Atmos. Sci.* **29**, 497.

KUO, H. L. 1963 *Phys. Fluids* **6**, 195.

LANCE, G. N. & ROGERS, M. H. 1962 *Proc. Roy. Soc.* A **266**, 109.

LILLY, D. K. 1966 *J. Atmos. Sci.* **23**, 481.

MARTIN, R. S. & WILKINSON, J. H. 1968*a* *Numer. Math.* **12**, 349.

MARTIN, R. S. & WILKINSON, J. H. 1968*b* *Numer. Math.* **12**, 369.

MOLER, C. B. 1971 *Stanford Comp. Sci. Rep.* STAN-CS-71-196.

NIILER, P. P. & BISSHOPP, F. E. 1965 *J. Fluid Mech.* **22**, 753.

PARLETT, B. N. & REINSCH, C. 1969 *Numer. Math.* **13**, 293.

PICHA, K. G. & ECKERT, E. R. G. 1958 In *Proc. 3rd U.S. Nat. Cong. on Appl. Mech.* p. 791.

ROSSBY, H. T. 1969 *J. Fluid Mech.* **36**, 309.

SCHULTZ-GRUNOW, F. 1935 *Z. angew. Math. Mech.* **15**, 191.

STEWARTSON, K. 1953 *Proc. Camb. Phil. Soc.* **49**, 333.

TATRO, P. R. & MOLLO-CHRISTENSEN, E. L. 1967 *J. Fluid Mech.* **28**, 531.

VERONIS, G. 1959 *J. Fluid Mech.* **5**, 401.

VERONIS, G. 1966 *J. Fluid Mech.* **24**, 545.

VON KÁRMÁN, T. 1921 *Z. angew. Math. Mech.* **1**, 233.

WASOW, W. 1953 *J. Res. Nat. Bur. Stand.* **51**, 195.

WILKINSON, J. H. 1965 *The Algebraic Eigenvalue Problem*. Oxford University Press.

ZONDEK, B. & THOMAS, L. H. 1953 *Phys. Rev.* **90**, 738.